Automatic Detection of Stent Graft Markers in 2-D Fluoroscopy Images

Sabrina Reiml[1,2], Marcus Pfister[1], Daniel Toth[1,2], Andreas Maier[2], Matthias Hoffmann[2], Markus Kowarschik[1], Joachim Hornegger[2]

[1] Siemens Healthcare GmbH, Forchheim, Germany
[2] Pattern Recognition Lab, Friedrich-Alexander-University Erlangen-Nuremberg, Erlangen, Germany

Abstract. An abdominal aortic aneurysm (AAA) is a widening of the aorta which can lead to death if the aneurysm ruptures. To prevent a rupture, the AAA has to be repaired by open surgery or by endovascular aneurysm repair (EVAR). In the recent years, EVAR achieved more popularity. In the procedure, a stent graft is placed at the position of the aneurysm to exclude it from the direct blood flow. The stent graft has to be positioned very precisely to prevent occlusion of the renal arteries. In advanced software tools, a segmentation of the aorta from computed tomography (CT) is available and the position of the two renal arteries is known. Their position is marked as an elliptical marker in the fluoroscopic overlay during the intervention. This paper describes a method to automatically detect stent graft markers to provide a second elliptical marker derived from the current stent position only. This helps the physician to get a comparison between the planned and the current position of the stent graft. The recall of the marker detection is 92% and the sensitivity is 96%. For the center of the fitted object we get a mean error of 1.60±1.69 mm.

Keywords: fast radial symmetry transform, ellipse fitting, abdominal aortic aneurysm, EVAR

1 Introduction

An abdominal aortic aneurysm (AAA) is a lasting and irreversible localized dilation of the aorta by a minimum of 50% of its diameter [9]. Due to the aging population, AAAs are becoming more common. The incidence of AAAs in men older than 60 years is between 4.1% and 14.2% and is much higher than in women, where the probability ranges from 0.35% to 6.2% [3]. The rupture risk is proportional to the diameter of the aneurysm. The mortality rate, if the aneurysm ruptures, ranges from 65% to 85%. Half of the patients die on the way to hospital [2,11,13]. As aneurysms are asymptomatic, they are found accidentally by other examinations, e.g., during a radiography of the prostate gland or an ultrasonography (US) of the kidneys.

If the diameter of the aneurysm is larger than 5.5 cm, it is recommended to be repaired. The aneurysm can be repaired by open surgery or by endovascular aneurysm repair (EVAR) [9]. During surgical repair, the whole abdomen is opened. The disadvantage of this procedure is the high operation risk. After the surgery, patients have to stay long in the hospital. The newer approach is EVAR. This intervention is a less invasive method compared to open surgery [5]. Catheters are inserted through the femoral arteries and a stent graft is placed at the position of the aneurysm. The procedure is guided by fluoroscopic imaging [9,12]. During the intervention, contrast agent is injected to visualize vascular structures clearly. However the renal function of older patients may not be sufficient to process the contrast medium. Thus it is desirable to use as little agent as possible.

A more novel workflow for the EVAR procedure is to register a segmented preoperative computed tomography (CT) Angiogram to the C-arm system [10]. In an overlay image, 3-D information of the segmented CT is fused with 2-D X-ray images. The segmented aorta, its branching arteries and corresponding guiding Landmarks (LMs) are projected onto the fluoroscopic image. LMs are provided automatically by the segmentation. The ostia of the two renal arteries are marked by circular LMs. The landing zone below the lower renal artery is provided by a LM, a ring in the aortic wall. The stent graft has to be positioned below the two renal arteries, in order not to occlude them. This gives the physician additional 3-D guidance for positioning the stent graft, which may lead to reduction in contrast agent. For infra-renal cases, the small radiopaque markers defining the start of the covered part of the stent graft can be aligned with this landing zone, see Figure 1.

Previously, Volpi et al. introduced a method to automatically detect and track a stent graft delivery device. The approach is based on the Robust Principal Component Analysis [15]. Demirci et al. suggest to automatically match a 3-D model of the stent graft to an introperative 2-D image, in which the device is shown. It is based on automatic preprocessing and a global-to-local registration [4].

In this paper, the detection of the stent graft markers by using fast radial symmetry is presented [8]. To get a comparison between the planned landing zone and the stent graft, the markers are connected to an ellipse or to a line to support the physician by positioning the stent at the correct position. The evaluation shows that the markers are detected robustly and the correct ellipse or line is suggested.

2 Methods

Our proposed method consists of three steps: first, possible stent graft markers are detected in the fluoroscopic image. Using the registered 3-D segmentation of the aorta, outliers are rejected and groups of markers belonging together are identified. Finally, a single group of markers is selected and, depending on the geometry of the points, an overlay depicting a line or an ellipse is generated.

2.1 Marker Detection

The position of the markers is detected by the fast radial symmetry transform [1,8], which detects radial symmetric objects in the images. The radial symmetry is determined by analyzing image gradients. For a given radius n, a pixel $\boldsymbol{p}_{+ve}(\boldsymbol{p})$ is called positively affected by the pixel $\boldsymbol{p}$, if the distance between $\boldsymbol{p}_{+ve}(\boldsymbol{p})$ and $\boldsymbol{p}$ is n and the gradient $\boldsymbol{g}(\boldsymbol{p})$ is pointing towards $\boldsymbol{p}_{+ve}(\boldsymbol{p})$. It is determined by

$$\boldsymbol{p}_{+\mathrm{ve}}(\boldsymbol{p}) = \boldsymbol{p} + \mathrm{round}\left(\frac{\boldsymbol{g}(\boldsymbol{p})}{||\boldsymbol{g}(\boldsymbol{p})||}n\right). \quad (1)$$

A pixel $\boldsymbol{p}_{-ve}(\boldsymbol{p})$ is called negatively affected if the gradient is pointing away from it. Pixels which are affected by a relatively large number of gradients are likely centers of radial symmetric objects. It is proposed to repeat this for several radii n, however, in our case the expected radius is known from the actual marker size and the C-arm camera geometry. The two closest integer values, the nearest lower and the nearest higher value of the expected radius, are used as radii to be sure to detect all markers. As the markers appear dark in the image, we can also limit us to positively affected pixels.

For the center detection of the marker area in the image, connected components labeling on the thresholded images is used [7]. The threshold is chosen heuristically, as a certain percentage of the maximum pixel intensity in the image.

2.2 Selection of Stent Graft Markers

By the marker detection in the X-ray image, other objects which are no stent graft markers are detected. These can be other markers in the stent or in the background. To localize the stent graft markers, the information of the LM from the registered segmentation is used. The center of the 3-D ellipse representing the LM, which corresponds to the center of the aorta, is projected into the X-ray image. Due to the anatomy of the patient and the viewing directions used in EVAR procedures, a vertical search space around the projected center point can be created for the stent graft markers, see Figure 1. This corresponds to the anatomy of the aorta in which the stent graft is located. The width of the searching area h_x is the known width of the aorta. The orange dotted rectangle is used as a sliding window and for each window an ellipse or line is computed, if markers are detected.

2.3 Line and Ellipse Fitting

If only one marker is detected, no line or ellipse can be fitted. For two markers, a line is fitted, for more than two markers, the distance of the markers to the regression line is calculated. If all distances are equal or less than two pixels, the regression line is the solution, otherwise the ellipse is the result.

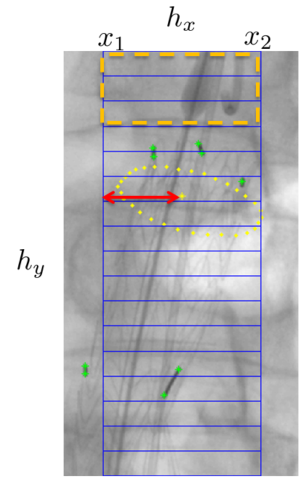

Fig. 1. Sliding window details: x_1 and x_2 are the borders of the sliding window. The width is h_x, the height of the area where the window is sliding down is h_y. The red arrow is the distance between the center of the landmark which is below the two renal arteries and the left border of the sliding window. The orange dotted rectangle is the window which is sliding down.

2.4 Decision for the right solution

As not only stent graft markers are detected but also other false positives, a sliding window is used which contains a part of the markers. For each window, a line or an ellipse is fitted, dependent of the number and position of the markers. For connecting the markers to a line, singular value decomposition (SVD) is used to solve the line equation [14]. A given set of n line points (x_i, y_i), where $i = 1, ..., n$, have to fulfill the equation $y_i = mx_i + t$. The parameter m represents the slope and t represents the intercept of the line. For the connection of the found markers to an ellipse, the Numerically Stable Direct Least Squares Fitting of Ellipses by Halíř et al. [6] is used.

For each window we get one solution, in the end there may be several lines and ellipses given. There are three cases: only lines, only ellipses or lines and ellipses. To select the correct line or ellipse, a decision tree is used. The decision tree, if ellipses and lines are given, is shown in Figure 2. The center of an ellipse is denoted by (c_x, c_y). The rotation angle of an ellipse with respect to the horizontal axis is denoted by γ. The slope of the line is m. If only lines are given, the right part of the decision tree is used. If only ellipses are given, the first decision is to delete all ellipses with the same center and then, if two or less ellipses remain, the ellipse with the smaller rotation angle γ is chosen because for repairing the AAA, the main direction of stent placement is vertical. If more than two ellipses remain, the ellipse in the lowest window is chosen as the stent is inserted from the bottom.

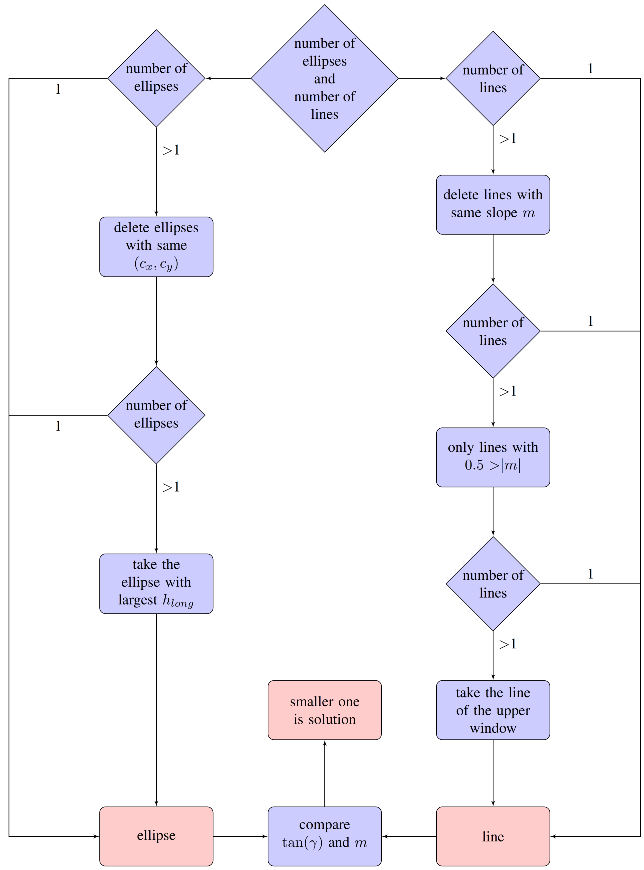

Fig. 2. Decision process, whether ellipse or line to be chosen.

3 Results and Evaluation

3.1 Data Description

For the evaluation, X-ray images were provided by two clinical collaboration sites, Centre Hospitalier de l'Université de Montréal (CHUM) and Universitätsklinikum Heidelberg (HD). The evaluation was performed on 7 patients from CHUM and 13 patients from HD, altogether on 63 frames.

3.2 Detection of Markers

For the detection of the markers, several parameters have to be chosen. There are different stents, which have different marker sizes and forms. The radii of the markers, which should be detected is set to four and five pixels in case of using Endurant and Gore Excluder C3 stent grafts. In case of Zenit Flex and Zenith LP

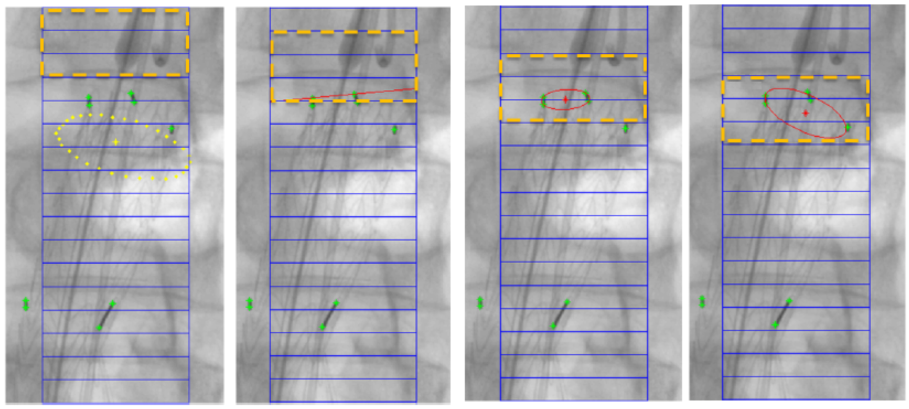

Fig. 3. Sliding window (dotted orange) inside a certain area (blue) to fit an ellipse or line to the markers. The green crosses represent the found markers and the yellow dotted ellipse is the landmark of the two renal arteries.

devices, the radii are set to two and three pixels. The radius is set to two values to increase the robustness of marker detection. To decrease the computation time, only positively affected pixels are examined and small gradients are neglected. For the evaluation, the detection results are categorized into four groups:

- True Positive (TP)
- False Positive (FP)
- False Negative (FN)
- True Negative (TN).

The stent graft markers, which are detected correctly, are categorized as TP. Markers, which are not found are FN. TN are other, nonrelevant markers which are found, but not used for the ellipse fitting. The pixels, which are detected wrongly as markers and which are used for the ellipse or line fitting are FP.

The 63 frames which are used for the evaluation contain 314 stent graft markers which should be detected. The detection result is presented in Table 1. The detection result is measured with recall and precision. The recall and precision are calculated as

$$recall = \frac{TP}{TP + FN} = \frac{290}{290 + 24} = 0.92 \tag{2}$$

and

$$precision = \frac{TP}{TP + FP} = \frac{290}{290 + 11} = 0.96. \tag{3}$$

3.3 Ellipse or Line Fitting

To fit an ellipse or a line and to localize the markers, a sliding window is used, see Figure 1. The position of the landmark (yellow ellipse) at the position of

True Positive	290
True Negative	226
False Positive	11
False Negative	24

Table 1. Marker detection results for all data.

the two renal arteries is given as a ring, as illustrated in Figure 3. The width h_x of the window is 240 pixels because this corresponds to the diameter of the aorta with an additional safety margin, see Figure 1. The height h_y of the window is the height of the image. The vertical shift of the sliding window is $1/3 \cdot \Delta y$ where $\Delta y = h_y/9$. The ground truth is performed by manual annotations. The markers are selected manually and for the ellipse, the center, the long axis, the short axis and the angle of rotation are set. For the calculation of the 2-D error of the detected centers, the Euclidean distance $\epsilon = \|\boldsymbol{q}_c^* - \hat{\boldsymbol{q}}_c\|_2$ is computed, where $\boldsymbol{q}_c^*$ depicts the ground truth and $\hat{\boldsymbol{q}}_c$ is the estimate. To evaluate the long half axis, the short half axis and the rotation angle, the difference (2-D error) between the ground truth and the result of the algorithm is calculated. For the center, we achieve an error of 1.60 ± 1.69 mm (7.40 ± 6.96 pixels). The median is 1.08 mm (4.88 pixels). For the long half axis, we get an error of 1.86 ± 2.39 mm (7.85 ± 8.43 pixels). The median of the difference of the long half axis is 1.09 mm (5.18 pixels). For the short half axis, we get an error of 0.62 ± 0.98 mm (3.33 ± 5.16 pixels). The median of the difference of the short half axis is 0.22 mm (1.06 pixels). For the rotation angle, we get an error of 6.23 ± 5.55 degrees. The median of the difference of the rotation angle is 5.07 degrees.

4 Conclusion

This paper proposes an approach for automatic stent graft marker detection during endovascular AAA repair. The marker detection is robust, with a recall of 92 % and a precision of 96 %. Although not all markers are found, the ellipse or line fitting is robust, shown by the mean error of the center of 1.60 ± 1.69 mm. The presented method is limited to abdominal EVAR, since it is not able to detect rotated stents.

The following research direction is to find markers of a fenestrated stent and to mark the area, to which branching artery the markers correspond. Another research direction is to use learning based methods instead of the decision tree for the correct decision for the line or for the ellipse.

Acknowledgements and Disclaimer. The authors gratefully acknowledge the help of the group of Prof. Dr. med. D. Böckler from HD and the group of Dr. G. Soulez MD, Msc from CHUM for providing the clinical data. The concepts and information presented in this paper are based on research and are not commercially available.

References

1. Berger, M., Forman, C., Schwemmer, C., Choi, J.H., Müller, K., Maier, A., Hornegger, J., Fahrig, R.: Automatic Removal of Externally Attached Fiducial Markers in Cone Beam C-arm CT. In: Deserno, H.H.T. (ed.) Bildverarbeitung für die Medizin 2014. pp. 168–173 (2014)
2. Budd, J.S., Finch, D.R.A., Carter, P.G.: A Study of the Mortality from Ruptured Abdominal Aortic Aneurysms in a District Community. European Journal of vascular surgery 3(4), 351–354 (1989)
3. Cornuz, J., Pinto, C.S., Tevaearai, H., Egger, M.: Risk factors for asymptomatic abdominal aortic aneurysm: Systematic review and meta-analysis of population-based screening studies. The European Journal of Public Health 14(4), 343–349 (2004)
4. Demirci, S., Bigdelou, A., Wang, L., Wachinger, C., Baust, M., Tibrewal, R., Ghotbi, R., Eckstein, H.H., Navab, N.: 3d stent recovery from one x-ray projection. In: Medical Image Computing and Computer-Assisted Intervention–MICCAI 2011, pp. 178–185. Springer (2011)
5. Egorova, N., Giacovelli, J., Greco, G., Gelijns, A., Kent, C.K., McKinsey, J.F.: National outcomes for the treatment of ruptured abdominal aortic aneurysm: Comparison of open versus endovascular repairs. Journal of vascular surgery 48(5), 1092–1100 (2008)
6. Halíř, R., Flusser, J.: Numerically Stable Direct Least Squares Fitting of Ellipses. In: Proc. 6th International Conference in Central Europe on Computer Graphics and Visualization. vol. 98, pp. 125–132. Citeseer (1998)
7. Jankowski, M., Kuska, J.P.: Connected components labeling–algorithms in Mathematica, Java, C++ and C#. In: Fiala, J., Koubek, V., Kratochvíl, J. (eds.) New Ideas in Symbolic Computation: Proceedings of the 6th International Mathematica Symposium (2004)
8. Loy, G., Zelinsky, A.: Fast Radial Symmetry for Detecting Points of Interest. IEEE Transactions on Pattern Analysis and Machine Intelligence 25(8), 959–973 (August 2003)
9. Nevala, T.: Endovascular Treatment of an Abdominal Aortic Aneurysm - Mid-Term Results and Management of a Type II Endoleak. Ph.D. thesis, University of Ouluensis (2010)
10. Pfister, M., Toth, D.: Clinical Prototype of an integrated Workflow for EVAR using Surface Meshes of pre-operative CT data. In: Proceedings of IGIC 2014 (2014)
11. Sakalihasan, N., Limet, R., Defawe, O.D.: Abdominal aortic aneurysm. The Lancet 365(9470), 1577–1589 (2005)
12. Tangen, G.A., Manstad-Hulaas, F., Brekken, R., Hernes, T.A.: Aortic Aneurysm-Recent Advances, Chapter 5: Navigation in Endovascular Aortic Repair. InTech (2013)
13. Thompson, M.M.: Controlling the expansion of abdominal aortic aneurysms. British journal of surgery 90(8), 897–898 (2003)
14. Tomasi, C.: CS 296.1 Mathematical Modelling of Continuous Systems. Duke University (2004)
15. Volpi, D., Sarhan, M.H., Ghotbi, R., Navab, N., Mateus, D., Demirci, S.: Online tracking of interventional devices for endovascular aortic repair. International Journal of Computer Assisted Radiology and Surgery pp. 1–9 (2015)